Available online at www.sciencedirect.com
SCIENCE DIRECT®
Progress in Biophysics and Molecular Biology 90 (2006) 378–398
Progress in Biophysics & Molecular Biology
www.elsevier.com/locate/pbiomolbio

Review

Phase singularities and filaments: Simplifying complexity in computational models of ventricular fibrillation

R.H. Clayton[a,*], E.A. Zhuchkova[b], A.V. Panfilov[c]

[a]*Department of Computer Science, University of Sheffield, Regent Court, 211 Portobello Street, Sheffield, S1 4DP, UK*
[b]*Physics Faculty, Moscow State University, Russia*
[c]*Department of Theoretical Biology, University of Utrecht, The Netherlands*

Available online 25 July 2005

Abstract

In the whole heart, millions of cardiac cells are involved in ventricular fibrillation (VF). Experimental studies indicate that VF is sustained by re-entrant activity, and that each re-entrant wave rotates around a filament of phase singularity. Filaments act as organising centres, and offer a way to simplify and quantify the complex spatio-temporal behaviour observed in VF. Where a filament touches the surface of fibrillating myocardium re-entrant activity can be observed, however the behaviour of filaments within bulk ventricular myocardium is difficult to observe directly using present experimental techniques. Large scale computational simulations of VF in three-dimensional (3D) tissue offer a tool to investigate the properties and behaviour of filaments, and the aim of this paper is to review recent advances in this area as well as to compare recent computational studies of fibrillation in whole ventricle geometries.

Keywords: Computer model; Re-entry; Ventricular fibrillation; Phase singularity; Filament

Contents

*Corresponding author. Tel.: +44 114 222 1845; fax: +44 114 222 1810.
E-mail address: r.h.clayton@sheffield.ac.uk (R.H. Clayton).

0079-6107/$ - see front matter © 2005 Elsevier Ltd. All rights reserved.
doi:10.1016/j.pbiomolbio.2005.06.011

1. Introduction

Sudden death resulting from ventricular fibrillation (VF) is an important healthcare problem in the industrialised world (Huikuri et al., 2001; Priori et al., 2001). VF is characterised by asynchronous contraction of the heart and it is widely accepted that this type of contraction results from a turbulent pattern of heart excitation. The mechanisms that organise and sustain excitation patterns during VF and other cardiac arrhythmias remain poorly understood; yet have fascinated scientists and clinicians for many years (Surawicz, 2003; Surawicz, 2004). Early experiments showed that a ring of tissue cut from either the atria or the ventricles could support a circulating excitation (Garrey, 1914; Mines, 1914), and later studies in intact hearts found activation sequences during VF that were consistent with this re-entrant mechanism (Lewis, 1925; Wiggers, 1940). During re-entry electrical activity propagates repeatedly along a closed path, forming a spiral wave of activation in two dimensions (2D) and a scroll wave in three dimensions (3D). Studies using high-resolution epicardial mapping with multiple electrodes (Frazier et al., 1989; Janse et al., 1980; Kim et al., 1997; Lee et al., 1996; Rogers et al., 1999) and voltage-sensitive fluorescent dyes (Choi et al., 2001; Gray et al., 1998; Samie et al., 2001; Witkowski et al., 1998) have assembled abundant experimental evidence to support the idea that the dominant mechanism sustaining VF is re-entry.

Over 80 years ago, two types of re-entry that could sustain VF were first discussed (Lewis, 1925), and the mechanism is still a topic of active debate and investigation (Chen et al., 2003; Panfilov and Pertsov, 2001; Rogers and Ideker, 2000). Two types have been proposed. In the first, VF is sustained by a single fast re-entrant wave or mother rotor (Lewis, 1925), which may be either stationary (Samie et al., 2001) or mobile (Gray et al., 1995), and may induce secondary turbulent wave patterns by interaction with cardiac tissue heterogeneities. In the second, the excitation pattern during VF is organised by multiple re-entrant wavelets (Choi et al., 2002; Lee et al., 2001; Moe et al., 1964). These two perspectives are not mutually exclusive, and recent data have shown that both types of VF can exist in isolated rabbit hearts (Wu et al., 2002).

For physical scientists and engineers, models offer a quantitative framework for organising ideas about system behaviour. In cardiac research, mathematical and computational models have

become an increasingly important research tool, and this development has been driven by increases in both computational power and availability of experimental information. Although patterns of electrical activity during VF in the surface layer of experimental preparations can be observed with high spatial resolution using electrode arrays or voltage-sensitive fluorescent dyes (Efimov et al., 2004), similar measurements within the ventricular wall are extremely difficult to obtain (Barnette et al., 2000; Baxter et al., 2001). Thus experimental recordings of re-entry on the tissue surface typically show spiral waves, which are the surface (2D) manifestations of 3D scroll waves. Computational models of activation during VF have an important role because they can be used to propose 3D mechanisms that are consistent with 2D surface observations. A good analogy for this situation is study of the sun, where observations can only be made in a thin surface layer, and must be interpreted using a model-based understanding of stellar nuclear reactions.

Spiral waves and scroll waves are active sources of excitation, which organise the spatio-temporal pattern of excitation of myocardium during an arrhythmia. 2D spiral waves are characterised by a wavebreak at the core of the spiral (spiral wave tip). This is sometimes referred as a point of phase singularity (PS), because at this point the phase of the wave is undefined. 3D scroll waves are characterised by lines of phase singularity called filaments. Fig. 1 shows example spiral waves and scroll waves in a computational model of cardiac tissue, together with phase

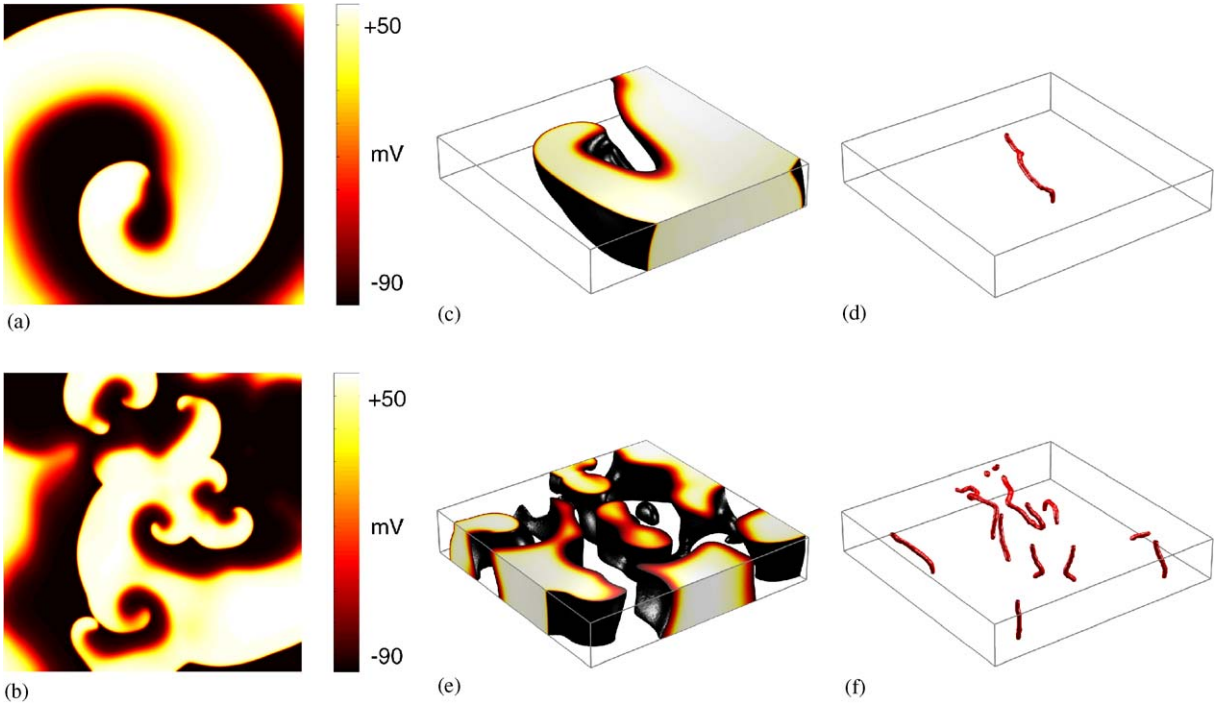

Fig. 1. Examples of 2D re-entry with a single spiral wave (a), and multiple spiral waves (b). Examples of 3D re-entry with a single scroll wave (c) and a single filament (d), and with multiple scroll waves (e), with multiple filaments (f). All the simulations depicted used the three-variable Fenton–Karma model.

singularities and filaments. During VF the end of one or more filaments may touch the tissue surface and be manifest as a spiral wave. When more than one spiral wave (Fig. 1b) or scroll wave (Fig. 1e) is present, the pattern of spatio-temporal activity can be very complex because the activation waves interact. Decomposing the complex activation patterns to show filaments (Fig. 1f) provides information about how many sources organise the excitation pattern, and tracking them will explain the changes in the excitation pattern in the course of time. Understanding the laws governing filament dynamics can give us a key for understanding the mechanisms of cardiac arrhythmias, because the overall excitation pattern can be found by adding the pure geometrical motion of waves around filaments.

In order to apply this approach practically, we need algorithms for identification of filaments from 3D wave propagation patterns, and we need to understand the laws for filament dynamics in cardiac tissue. The aim of this paper is to review the current status of research in this area.

2. Computational models of cardiac tissue

We can distinguish the following levels of organisation in cardiac tissue: cellular, tissue and whole organ. At the cellular level, the excitability of a cardiac myocyte results from current flow through ion channels and transporters embedded in the cell membrane. The conductance of these proteins is generally voltage and time dependent, and so the electrical behaviour of the cell membrane can be described by a system of ordinary differential equations (ODEs). The current generation of cardiac cell models are based on the Hodgkin–Huxley model of the squid giant axon (Hodgkin and Huxley, 1952) first adapted for cardiac Purkinje cells by Noble (Noble, 1962). Based on these pioneering studies, a range of cardiac cell models have now been developed that embrace the many ion channels and transporters involved in generating the cardiac action potential (Noble and Rudy, 2001).

Cardiac tissue is composed of excitable cells that are coupled by gap junctions. The rod-like myocytes are generally aligned in parallel, and are closely packed in fibres and sheets whose orientation varies spatially (Nielsen et al., 1991; Streeter, 1979). Propagation is two to three times faster along fibres than across them, and fibre orientation changes by about 120° across the ventricular wall. Although propagation of an action potential from one myocyte to its neighbours depends on the properties of local gap junctions (Kleber and Rudy, 2004), large scale models of propagation assume that the electrical properties of cardiac tissue can be spatially averaged and described by conductivity tensors in two domains representing the extracellular and intracellular space (Henriquez and Papazogou, 1996). Thus, cardiac tissue can be modelled as a *biodomain*, using two partial differential equations (PDEs). If the conductivity tensors in the extracellular and intracellular space are proportional to each other, or if the resistance of extracellular space can be neglected, then cardiac tissue can be modelled as a *monodomain* where propagation is described by a single PDE.

At the whole organ level, anatomically detailed models have been developed for the porcine (Stevens et al., 2003), canine (Nielsen et al., 1991), rabbit (Vetter and McCulloch, 1998), and mouse (Henriquez et al., 2004) ventricles. These geometries can be used to construct a computational domain within which the propagation model be solved numerically. A variety of

finite difference and finite element schemes have been used to solve both monodomain and bidomain models (Beaumont et al., 1998; Fenton and Karma, 1998b; Keener and Bogar, 1998; Trayanova et al., 2002), but an extended discussion of numerical methods is beyond the scope of this paper.

3. Methods for identification of filaments

Filaments can be considered as lines of wavebreak around which a scroll wave rotates, and methods for detecting filaments aim to locate this wavebreak. For stationary or slowly drifting filaments wavebreaks can be found using spatial and temporal averaging methods (Mironov et al., 1996; Pertsov et al., 1993). These approaches rely on lower membrane voltage close to the filament, and assume that the timescale of filament motion is much less than the period of rotation. However, excitation patterns during VF are not stationary and hence there is a need for algorithms that can identify filaments from short sections of data. As the filament is defined by a wavebreak, at the filament the surfaces of activation and recovery intersect. In computational models these surfaces can be determined either explicitly or by transforming activation into phase as described in the next two sections.

3.1. Intersection of activation and recovery curves

In numerical simulations of re-entry information about both activation and recovery is available, and the intersection of activation and recovery curves has been used to locate phase singularity points in 2D (Biktashev and Holden, 1998; Krinsky et al., 1992), and 3D (Fenton and Karma, 1998b). A variant of this approach uses the magnitude of the cross product of gradient vectors for excitation and recovery, which reaches a maximum value close to the filament (Winfree et al., 1996). The activation curve can be an isoline or isosurface of constant membrane voltage (Fenton and Karma, 1998b), although activation of the Na^+ channel has also been used (Sambelashvilli and Efimov, 2004). For the recovery curve a line or surface of $dV_m/dt = 0$ (Clayton and Holden, 2002b; Fenton and Karma, 1998b), the gating variable for the Ca^{2+} channel (Biktashev and Holden, 1998), and inactivation of the Na^+ channel (Sambelashvilli and Efimov, 2004), have all been used. Fig. 2b and c illustrate the intersection of lines of constant voltage and $dV_m/dt = 0$ for the spiral wave shown in Fig. 2a.

3.2. Phase transformation

Isochrones of activation and recovery can also be considered to be lines of equal phase, where phase describes progress through the activation-recovery cycle. Cardiac tissue can therefore be represented in phase space, in which a recovery variable is plotted against activation and the activation-recovery process is associated with a closed loop trajectory (Gray et al., 1998). The progress of individual elements around this loop can then be described by a phase angle φ, which can be calculated from

$$\varphi(t) = a \tan 2(V_m(t) - V^*, R(t) - R^*),$$

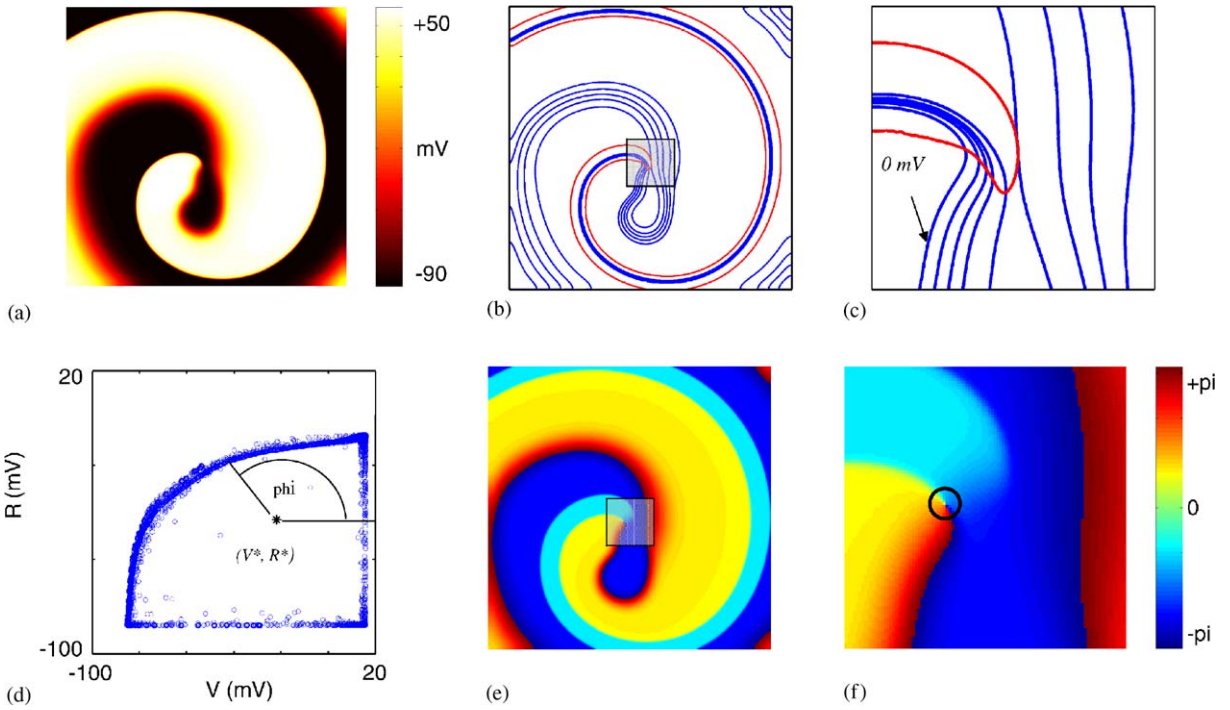

Fig. 2. Comparison of methods for identifying phase singularities. (a) Spiral wave in 6×6 cm tissue model with excitability described by the three-variable Fenton–Karma model. (b) Isolines of membrane voltage at 0, −20, −40, −60, and −80 mV (blue) and $\mathrm{d}V_\mathrm{m}/\mathrm{d}t = 0$ (red). (c) Close-up of central shaded region of (b), showing intersection of activation and recovery isochrones that identify phase singularity. (d) Phase portrait of points in (a), each blue circle indicates a grid point, and the phase of each point is calculated from the angle subtended by the point at the origin (V^*,R^*), which is shown as an asterisk. In this example V is membrane voltage, and R is membrane voltage with a time delay of 5 ms. (e) Phase transformation of (a). (f) Close up of central shaded region of (e) showing phase singularity point (black circle) surrounded by a complete cycle of phase.

where V_m is membrane voltage (activation), R is recovery, (V^*,R^*) is an origin, and $a\tan2$ is a four quadrant inverse tangent such that $\varphi(t)$ is in the range $[-\pi,\pi]$. There are several options for obtaining R. It is possible to use a variable associated with recovery, $\mathrm{d}V_\mathrm{m}/\mathrm{d}t$, or a Hilbert transform (Bray and Wikswo, 2002a) but the most widely used approach has been time-delay embedding of V_m (Bray et al., 2001; Iyer and Gray, 2001). For this approach, $R(t) = V_\mathrm{m}(t-\tau)$, where τ is a delay usually chosen to be between 2 and 30 ms (Bray and Wikswo, 2002b; Gray et al., 1998). Figs. 2d and e show the phase encoding for the spiral wave shown in Fig. 2a. Tissue in each phase of the activation-recovery cycle surrounds the spiral wave tip, but at the tip itself phase is undefined, and is a PS. Phase singularities can be located using algorithms that search for points surrounded by a complete cycle (Bray et al., 2001; Bray and Wikswo, 2002b; Iyer and Gray, 2001). Fig. 2f illustrates the phase portrait close to the tip of the spiral wave in Fig. 2a. Traversing any closed path that encloses the PS will involve moving through a complete phase cycle from $-\pi$ (blue) to π (red).

3.3. Comparison of intersection and phase methods

Both approaches can be implemented easily in numerical studies. Implementation of each method requires selection of several parameters, which require careful selection. For the intersection method these parameters are the critical value of activation, and the recovery parameter and its critical value. If the recovery parameter is chosen to be $dV_m/dt = 0$, then the time delay used to evaluate this condition must be determined. For most of the ionic models discussed in Section 2 this time delay should be around 2 ms to give a unique filament location (Clayton and Holden, 2002b).

In the phase method we need to define phase angle either from two state variables, or choose the time delay (τ) for time embedding if only voltage is used. In both cases we need to choose a reference point (V^*, R^*). Choice of these values is known to affect PS detection (Bray and Wikswo, 2002b; Iyer and Gray, 2001; Larson et al., 2003). They should be chosen so that the phase can be uniquely defined during the course of a spiral (scroll) wave rotation. The ideal reference point is one that is encircled by all trajectories. If one chooses a random point, this point may lie within some trajectories and outside others.

In most experimental studies voltage is the only state variable that can be obtained, and so application of the intersection and of the phase method require introduction of another state variable: $dV_m/dt = 0$, or time embedded voltage. In numerical studies the recovery curves for the intersection method and phase for the phase method can be found directly from state variables. However, in most numerical simulations the PS and filaments are defined from voltage data only, as simulations aim to relate their results to experimental recordings and hence use similar processing techniques. A systematic comparison of the different methods for filament identification and their implementation in the same simulation has not been performed yet, but is of great importance.

4. Properties of phase singularities and filaments

Both PS points and filaments are mobile, and their motion depends on electrophysiological properties of the tissue, as well as local parameter gradients, gradients in refractoriness, and tissue structure. Filaments in 3D tissue possess all the properties of PS points in 2D tissue, but filaments also possess additional properties that are conferred by the extra dimension and have no analogue for PS points.

4.1. Phase singularities

Dynamic and local gradients in refractoriness are established close to the tip of a spiral wave, and these cause the tip to meander in a trajectory, which can have a quite exotic shape (Zykov, 1986). In general, the shape of meander patterns changes from circular to Z and linear core as excitability increases (Efimov et al., 1995; Zykov, 1986), and may have complex dynamic behaviour (Qu et al., 2000; Winfree, 1991). In bidomain models the meandering patterns are even more complicated as they are additionally affected by the 4-fold symmetry of the equations (Roth, 2004). Phase singularities also move under the influence of neighbouring spiral waves

(Ermakova et al., 1989), and this PS interaction can be analysed as a particle-field problem (Bray and Wikswo, 2003). Gradients in APD can also cause phase singularities to drift with a component along the gradient and directed towards the region with longest APD, and another component perpendicular to the gradient (Aslanidi et al., 2003; Rudenko and Panfilov, 1983; TenTusscher and Panfilov, 2003).

4.2. Filaments

As we have already seen, a scroll wave is an extension of 2D spiral waves into 3D. The most simple scroll wave has a straight filament, and if the filament remains straight then this type of wave will behave as a 2D spiral. However, unlike a PS point a filament can be bent and twisted, and configuration and shape of the filament determines has an important influence on its behaviour and its interaction with other filaments.

4.2.1. Configuration and dynamical behaviour

Filaments organise a wave pattern in 3D. Given a filament configuration we can find the overall wave pattern by adding rotating waves around it. The fact that there is always a wave rotating around the filament also results in some topological constraints on possible filament configurations (Winfree and Strogatz, 1984). The most important restriction is that the filament can end only at the outer boundaries of cardiac tissue, or at an "inner" boundary by pinning to a heterogeneity within the myocardium. There must be a continuous cycle of phase around the filament, and this requirement results in the rules that pinning inside cardiac tissue is possible only for pair of counter rotating filaments, and that filaments cannot branch (Pertsov et al., 2000). A filament can also exist entirely inside the myocardium, but in that case it should be closed. Depending on their shape, filaments are usually described as **I**, **O**, or **U** shaped. **I**-shaped filaments touch opposite surfaces of the tissue and result in a spiral wave on each surface; in the ventricular wall an **I**-shaped filament would be transmural. **O**-shaped filaments form a closed ring, and produce activations on a single surface that are similar to those produced by repeated discharge of a focal source. A **U**-shaped filament is a partial **O**-shaped filament, with the broken ends touching the same surface and resulting in a pair of spiral waves. A variant of **U**-shaped filaments is one that touches two neighbouring surfaces of a tissue slab, for example the epicardial and cut surface of a piece of excised ventricular wall. Examples of each filament configuration are shown in Fig. 3.

In very general terms filament dynamics can be characterised by determining their number and shape. The number of filaments changes due to filament birth, death, amalgamation and bifurcation, usually called filament interactions. Examples of these interactions are shown in Fig. 3, and this approach has been used to quantify filament behaviour in simulations in both tissue slabs and whole ventricle geometries (Clayton and Holden, 2002a; Clayton and Holden, 2002b; Clayton and Holden, 2004a). Filament birth results from block of a wave. Filament death occurs when a filament moves to a boundary, or when an **O-** or **U**-shaped filament contracts below a critical radius. Filament amalgamation occurs when two filaments merge, and filament bifurcation occurs when two filaments split apart. An example of amalgamation is when an **O**-shaped filament and an **I**-shaped filament combine to form a curved **I**-shaped filament, and an example of bifurcation is when a looped **I**-shaped filament is pinched to form an **I**-shaped

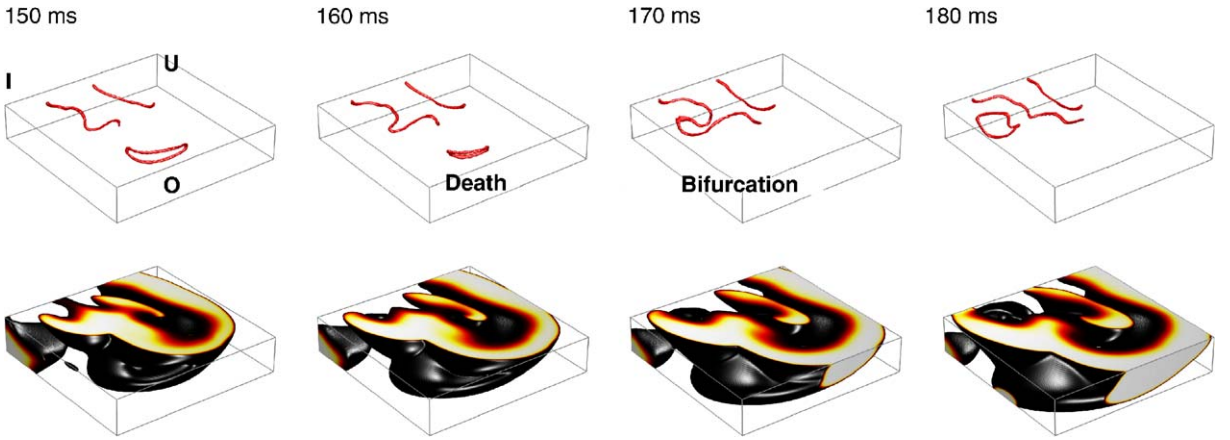

Fig. 3. Filament configuration and interactions in uniform anisotropic model with excitability described by the three variable Fenton–Karma equations (Clayton and Holden, 2002a, b). Top row; examples of **I**-, **U**-, and **O**-shaped filaments at 150 ms, contraction and death of **O**-shaped filament at 160 ms, and bifurcation of **I**-shaped filament at 170 ms to form new **I**- and **O**-shaped filaments.

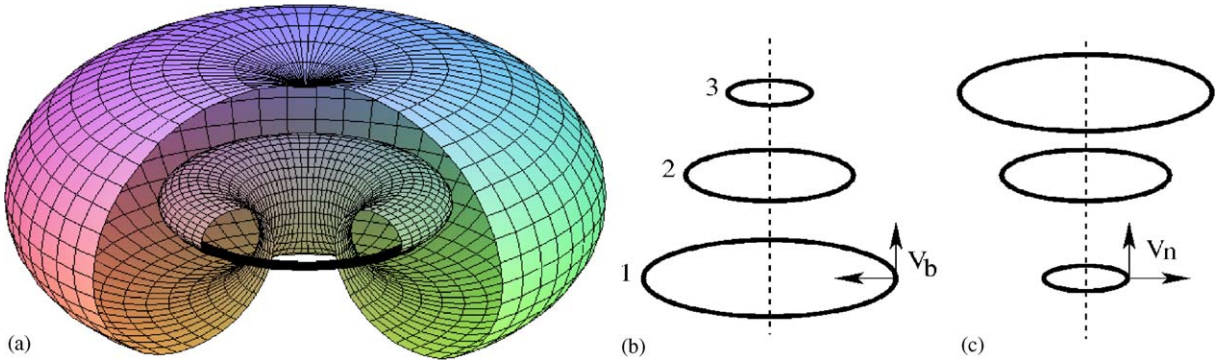

Fig. 4. Two regimes of scroll ring drift. (a) Scroll ring. (b) Contraction regime. (c) Extension regime.

and an **O**-shaped filament. Amalgamation and bifurcation may occur simultaneously when a pair of **I**-shaped filaments interact and form a pair of **U**-shaped filaments.

However filament interactions are not the only determinant of filament dynamics. Even single filaments have important dynamics resulting from their curvature and twist. Curvature and twist are purely 3D phenomena that do not have an equivalent in 2D. Curvature of the filament is just its geometrical curvature, while twist is the rate of change (the derivative) of the phase of re-entry along the filament.

4.2.2. Curvature

The effects of curvature on filament dynamics were first studied for scroll rings (Panfilov and Rudenko, 1987; Panfilov et al., 1986; Panfilov et al., 1984; Winfree, 1973). In these papers it was shown that the rotation of a scroll ring is non-stationary: the position of its filament is not stabilised and it drifts in space. Fig. 4 shows the dynamics of a scroll ring in a numerical

simulation with the FitzHugh Nagumo model. For the parameter values shown in Fig. 4b the filament contracted, and drifted upward. When the ring filament reached a critical radius, collapse of a scroll ring occurred. At other parameter values the filament was found to extend (Fig. 4c). Both drift velocities were inversely proportional to the filament curvature:

$$V_n = D_n k; \quad V_b = D_b k,$$

where V_n and V_b are drift velocities in normal (horizontal in Fig. 4a) and binormal (vertical) directions, D_n and D_b are proportionality coefficients, and k is filament curvature.

The most important component of the drift velocity is drift in the normal direction. It determines the change of filament length in time and has been called filament tension, with a positive tension referring to the contraction regime and a negative tension referring to the extension of the filament. With contraction the total length of a filament decreases, while with extension the total length of a filament increases. Tension therefore affects significantly the stability of a scroll wave filament in 3D, regardless of the filament shape. If the filament has positive tension and contracts, it will either collapse or will attain a stable shape, with the minimal possible length. For example in a rectangular slab of isotropic cardiac tissue it would evolve to a straight line orthogonal to the opposite tissue boundaries. This shape will be stable for perturbations, as any perturbation in this case will increase the filament length, and thus will result in a drift that returns the filament to the stable configuration (Biktashev et al., 1994). However, if the filament has negative tension it tends to increase its length, form loops and if they touch a tissue boundary, it will result in the filament breaking into two pieces, leading to filament multiplication and the onset of multiple wavelet VF (Alonso et al., 2003; Biktashev et al., 1994; Fenton et al., 2002). For cardiac cell and tissue models, the parameters that determine the sign of filament tension are unknown, however, positive tension occurs for a medium with a high excitability while the negative tension occurs for a medium with a low excitability (Alonso et al., 2003; Cherry and Fenton, 2004; Panfilov and Rudenko, 1987).

A key question for cardiac researchers is the tension of filaments during re-entry in the heart. In the absence of other effects negative tension would favour unstable re-entry and VF, whereas positive tension would favour either tachycardia resulting from stable re-entry with a single filament or self-terminating arrhythmias resulting from short-lived filaments that shrink and collapse. For simplified models of cardiac excitability both positive as well as negative filament tension have been found (Gray and Jalife, 1998; Panfilov and Holden, 1993), but filament tension in ionic models for cardiac tissue has not been studied in detail. Our preliminary results show that in the Luo–Rudy phase 1 model (Luo and Rudy, 1991) for most parameter values the filament of the scroll wave contracts and a small extension of the filament can be obtained only with severe modifications of sodium current (Alonso, Panfilov, not published).

4.2.3. Twist

Twisted scrolls arise naturally in inhomogeneous media where the scroll filament is directed along the inhomogeneity. The rotation of a scroll wave in a 3D excitable medium consisting of two layers with different properties was studied by Panfilov et al. (1984). The period of scroll rotation in the lower layer T1 was shorter than the period of scroll rotation in the upper layer T2. Because of faster rotation in the lower layer, the scroll wave in the upper layer became twisted.

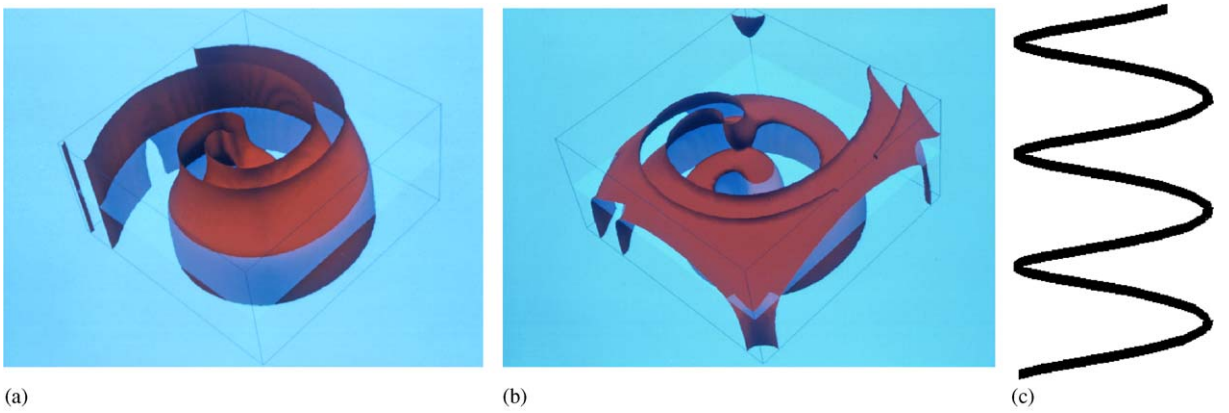

Fig. 5. Scroll wave in a heterogeneous medium, (a) twisted scroll; (b) scroll wave after the break (from Panfilov and Keener (1993a, b), with permission). (c) Helical scroll wave filament.

This twisting decreased the period of scroll wave rotation in the upper layer until this period became close to T1, when a stationary rotating scroll wave occurred. This scroll rotated with period of rotation close to the smaller natural period of the two media (T1). It was untwisted in the layer with natural period T1 and twisted in the layer with natural period T2 (Fig. 5a). Thus, the faster scroll drove the whole medium with period T1. If, however, the slower medium was not able to support scroll waves with the period of the faster medium, the scroll wave broke into two scrolls rotating independently in the lower and upper layers (Panfilov and Keener, 1993a). Eventually, the faster scroll eliminated the slower one and finally the whole medium was driven by the fast scroll wave (Fig. 5b). However, the periods of excitation in this case remained different: T1 in the lower layer and a slower period in the upper layer. Twist can also induce 'sproing' of a straight filament into radially expanding helices (Fig. 5c) as shown by (Henze et al., 1990; Storb et al., 2003).

In cardiac tissue, heterogeneity is distributed in space and has a gradient character. Gradients of action potential shape and duration exist both transmurally across the ventricular wall and from base to apex (Antzelevitch et al., 1991; Efimov et al., 1996; Wolk et al., 1999). Since APD determines in part the period of re-entry, filaments in the heart would be expected to accumulate twist from these gradients. Simulations in a slab of cardiac tissue using a simplified model have shown breakup of a scroll wave with transmural filament in a medium with a linear change in action potential duration between epicardial and endocardial surfaces (Clayton and Holden, 2003). Preliminary studies using a biophysically detailed ionic model scaled to reflect the transmural heterogeneity in APD found in real hearts show similar behaviour and suggest that this mechanism could exert a destabilising influence on re-entrant waves with transmural filaments during VF (Clayton and Holden, 2004b).

Scroll waves with gradient heterogeneities have also been studied in chemical excitable media, where an accumulation of twist leading to filament instability has been observed when a heterogeneity (temperature gradient) was directed along the filament (Mironov et al., 1996; Storb et al., 2003).

4.2.4. Anisotropy

If the fibres in cardiac tissue are straight and parallel to each other, anisotropy in monodomain equations can be removed by rescaling the coordinate system and will have no effect on scroll wave dynamics. However, the rotational anisotropy of the ventricular wall is not rescalable and can substantially affect filament behaviour in two ways. First, transmurally oriented filaments can twist, and second, filaments tend to align with fibre direction. We discuss each effect in turn.

The effect of rotational anisotropy on transmural filaments has been investigated in several numerical studies. An early study of scroll waves in an anisotropic model (Panfilov and Keener, 1995b) showed asynchronous fast and slow propagation of the re-entrant wave on endocardium and epicardium as the wavefront propagated along and across fibres, resulting in instability of the re-entrant wave. More recent studies have focussed on the filament, and have shown that rotational anisotropy causes asynchronous accumulation and dissipation of filament twist as the wave rotates (Clayton and Holden, 2003; Fenton and Karma, 1998a; Fenton and Karma, 1998b). These studies have also confirmed that rotational anisotropy can destabilise a filament if the ventricular wall exceeds a critical thickness or if a parameter gradient exists. The mechanism of instability is local accumulation of twist, which travels along the filament causing it to expand and bend. If a loop of the extended filament touches a surface, then the filament breaks. Other studies using detailed ionic models have indicated that APD restitution can play an important role in destabilising the filament (Qu et al., 2000), and that the shape of the meander pattern also exerts a significant influence on whether a filament is destabilised or not (Rappel, 2001).

For parameter values where breakup does not occur, rotational anisotropy causes the drift of spiral (scroll) waves (Panfilov and Keener, 1993b), and this drift results in alignment of the filament along fibres, if they are straight (Berenfeld and Pertsov, 1999). After becoming aligned with the fibres, the filament drifts in space minimizing its length (for positive filament tension) and finally attains a stable configuration. If the fibres are curved, the filament also attains a stable configuration, but it does not follow the fibres anymore (Fig. 6a). To predict this configuration Wellner et al. (2002) proposed a minimal principle for scroll wave filaments.

They showed that the stable filament shape of a scroll wave in a 3D anisotropic medium is given by a geodesic in a 3D space with a metric given by the inverse diffusivity tensor of the medium, thus providing an elegant analytical formulation for predicting stable filament shapes. This method was further developed in TenTusscher and Panfilov (2004), who were able to reformulate it using the equation describing wave propagation in the same medium in which the scroll wave rotates. They showed that the filament actually follows the path of the line along which the travel time of the wave is minimal. This formulation allows the application of wave algorithms for predicting filament shapes, which are much more effective than the solution of the geodesic equation. This formulation also allows prediction of the position of the filament in a domain of any shape and even without a priori knowledge of the position of filament ends on boundaries and of the anisotropy tensor of the medium, provided that wave arrival times can be found. Therefore this method could be applied for predicting filament shapes in experimental preparations. Fig. 6b shows results of such alignment for the case when there is a family of shortest travel time curves (the green surface). The red and the blue filaments show the result of time evolution of the filaments of the scroll waves initiated from different initial conditions. It can be seen that in the course of time both filaments align with the predicted minimum surface. In the case of a single

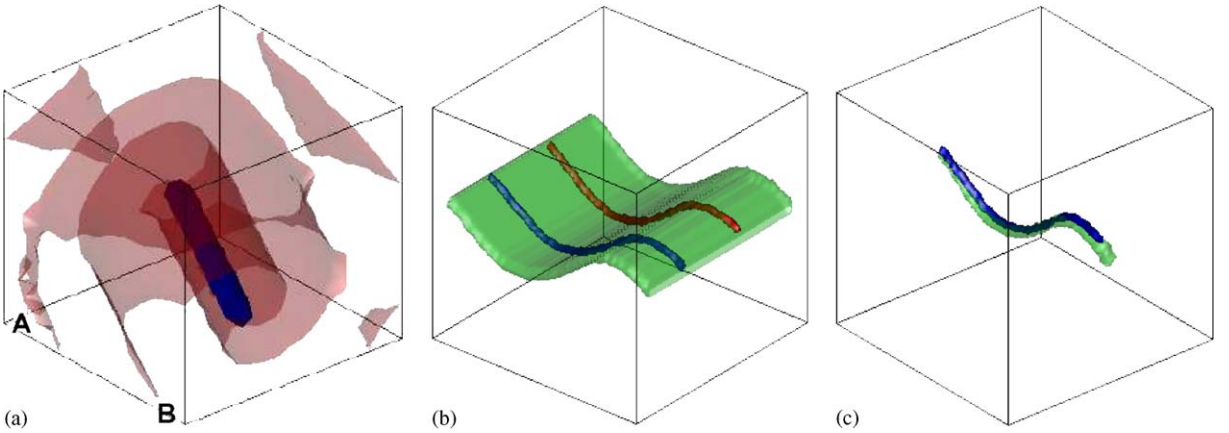

Fig. 6. Alignment of filament with fibres in computations in 3D cube with excitation described by the modified Aliev–Panfilov model with $a = 0.05$. (a) Filament (blue) and excitation wavefront (red) for simulation where fibres make an angle of 30° with the direction AB. (b,c) Stable filament shapes in anisotropic cardiac tissue. Each image shows the predicted filament shape resulting from the shortest path algorithm in green and the actual filament alignment in red and blue (reprinted from TenTusscher and Panfilov (2004) with permission, Copyright by the American Physical Society).

global minimum shown in Fig. 6c (the green line), the filament (blue) aligns with the predicted minimum path curve from any initial conditions.

4.2.5. Stability

The mechanisms that determine whether a re-entrant wave is stable or unstable in cardiac tissue are important, but space restrictions preclude a detailed discussion here. Dynamical instability resulting from steep APD restitution has been studied in detail (Garfinkel et al., 2000; Karma, 1993), and in 2D this results in break up of a spiral wave into multiple wavelets. However many other mechanisms for break-up have also been observed and documented (Fenton et al., 2002), and under some conditions steep APD restitution is not associated with break-up (Cherry and Fenton, 2004). We have already considered 3D mechanisms that can contribute to filament instability: negative filament tension and accumulated twist resulting from parameter gradients or rotational anisotropy.

5. Filaments in whole ventricle models of VF

Finally, we illustrate application of this approach for quantification of VF in simulations with anatomically detailed ventricular geometry. The development of an anatomical model of the canine ventricles at the University of Auckland that includes a detailed description of fibre orientation (Nielsen et al., 1991) has resulted in a number of computational studies in which the 3D organisation of VF has been probed. These have included simulations of stable and unstable scroll waves (Gray et al., 1995; Panfilov and Keener, 1995a), a simulation based on cellular automata and synchronous concurrent algorithms (Holden et al., 1996), and a simulation of

normal beats and VF in canine ventricles with a conduction system (Berenfeld and Jalife, 1998). Other studies have used a rabbit ventricle model developed at the University of California at San Diego (Cherry and Fenton, 2004; Rogers, 2002). Three recent studies have focussed on the number and properties of filaments in the canine ventricular geometry (Clayton and Holden, 2004a; Panfilov, 1999; Xie et al., 2004). All these studies used the monodomain description of cardiac tissue, similar numerical methods for their integration (based on the explicit Euler method) and similar algorithms for filament identification (the intersection method). However, the equations for cardiac cells and spatial resolution of the models differed substantially.

In the first study, 3D organisation of VF was studied in the Auckland canine geometry using the simplified Aliev–Panfilov two-variable cell model (Panfilov, 1999). VF was modelled as a process of scroll wave breakup and the number of filaments sustaining VF was measured. On average the VF was organized by 38 ± 4.85 filaments and the total length of the filaments was 1450 ± 106 mm. The average length of the filament was thus 38 mm, which is about two times longer than the maximal thickness of myocardial wall in this model. This indicated that the filaments in general were not aligned along a straight transmural line but were curved. If the size of the ventricular geometry was reduced the number of filaments rapidly decreased, and could be approximated by a power law with an exponent of 2.21 ± 0.034. The fact that the exponent was close to 2 indicated that in this model the filaments were mainly competing for the surface area of the heart.

The second of these studies (Clayton and Holden, 2004a) used the three-variable cell model developed by Fenton and Karma with parameters set to reproduce the steep APD restitution of the Beeler Reuter model (Fenton and Karma, 1998b). It was found that the average number of filaments fluctuated around a value of 36. The average filament length was 30 mm resulting in the total length of all filaments of approximately 1080 mm.

In the third study (Xie et al., 2004), VF dynamics in the Auckland canine anatomy model were studied using the Luo Rudy phase I model for cardiac tissue. Again, the number of filaments increased following scroll wave breakup before saturating. Between 600 and 1600 ms the average number of filaments was 40 while between 1000 and 1600 ms the average number was 55. The filaments were distributed proportional to the volume of the heart ventricles: the left ventricle which has a volume approximately three times larger than the right ventricle had on average three times more filaments. The data on the average and total filament length were not presented.

Comparing the results of these three studies we can conclude that all of them show a large number of filaments organizing VF (Fig. 7b–d). The total number of filaments sustaining VF in all studies are in reasonable agreement in spite of the different cell models used, indicating that the number of filaments is mainly determined by the geometrical characteristics of cardiac tissue such as size of the ventricles and the wavelength of re-entry (product of APD and conduction velocity), which were close in all these studies. The fact that the total filament number was close also indicates that the breakup in all models resulted in VF of similar complexity. However, tissue with a longer wavelength would be expected to support a smaller number of filaments, and more work is needed to quantify this possible effect.

In two of the studies (Clayton and Holden, 2004a; Xie et al., 2004) it was observed that around half of the filaments touched the epicardial surface, but that they were visible for much less than one rotation. This observation could account for the relatively low incidence of epicardial re-entry observed in experimental studies (Rogers et al., 1999). Furthermore, although the average

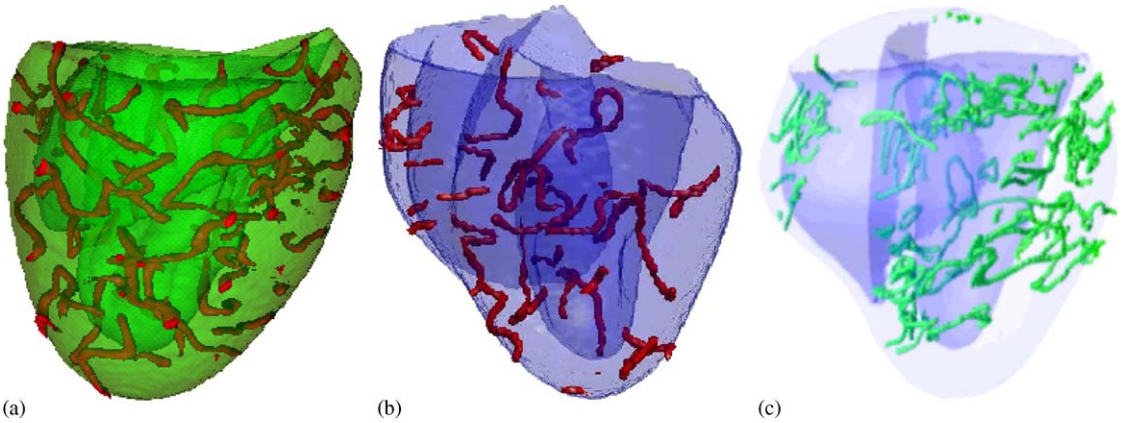

Fig. 7. Views of filaments during sustained multiple wavelet VF in the Auckland canine geometry with excitation described by (a) the Aliev–Panfilov model (reprinted with permission from Panfilov (1999), Copyright by the American Physical Society), (b) the three variable Fenton–Karma model (Clayton and Holden, 2004a, b), and (c) the phase I Luo–Rudy model (Xie et al., 2004).

filament length was about twice the thickness of the left ventricular free wall in two of the studies (Clayton and Holden, 2004a; Panfilov, 1999), some very long filaments were observed, and it is possible that these filaments became aligned with intramural fibres as suggested in an earlier study (Berenfeld and Jalife, 1998).

In the third study (Xie et al., 2004) the surface patterns during VF were quantified statistically. In a 3×3 cm area there were on average 1.6 and 2.0 wavelets in 1 s in the RV endocardium and epicardium, respectively, which for an equivalent mapping area in pig RV experiments reported 2.9 and 2.5 wavelets in 1 s, respectively (Valderrabano et al., 2002). The authors explain the differences by possible additional heterogeneities of the real heart.

In the studies reviewed in this section filaments were used as a tool for quantification of the excitation patterns during VF. The dynamics of individual filaments and possible effects of heterogeneity, anisotropy and twist on filament dynamics reviewed in Section 4 of this paper have yet to be addressed in anatomically detailed models of VF.

6. Limitations and future directions

In this review we have discussed how the spatio-temporally complex patterns of activation during VF are determined by filament behaviour, and shown how the dynamics and interaction of filaments in computational models of cardiac tissue is beginning to be understood. The story is not however complete. There are significant limitations to the work presented here, and important questions remain that should be addressed in future research.

Computational models must be carefully validated, and an appropriate model should be chosen to answer a particular research question. All models make assumptions. Most cardiac tissue models used to study filaments use simplified equations for excitability and ignore the effects of

calcium cycling and cardiac mechanics, which may have an important effect on re-entrant behaviour (Garny and Kohl, 2004; Nash and Panfilov, 2004). Furthermore most studies have used a monodomain model of cardiac tissue, although the more realistic boundary conditions that can be obtained with the bidomain model suggest that the type of boundary may affect filament behaviour close to the surface (Sambelashvilli and Efimov, 2004). Another study has also suggested that curvature of the epicardial surface could be an important factor for stability (Rogers, 2002).

A further limitation is the possible dependence of the results described here upon the type of models used. Most of the work reviewed here has used simplified models because 3D computations are computationally demanding, but are necessary to compute filament behaviour. One example of this problem is disagreement about the relative effect of rotational anisotropy, thickness, and APD restitution on filament stability (Fenton and Karma, 1998b; Qu et al., 2000). Another example is meander. In 2D simulations, the meander pattern of spiral waves varies greatly with both the cell model used, and the parameter settings. Most of the studies that have shown filaments aligning with fibre direction have used models with stable and non-meandering filaments. Although the main results are still expected to be valid for average filament positions, it is possible that meander can substantially affect the filament dynamics.

The questions raised in this review indicate some important future directions, and some of these can be summarised as follows:

- *Initiation*. The mechanisms by which re-entry can be initiated in 3D in both normal and abnormal (pathological) tissue need to be understood so that the most likely filament configuration for a given mechanism of initiation can be established, and its subsequent stability and behaviour predicted. So far only very limited studies in this direction have been performed (Aliev and Panfilov, 1996). The problem of re-entry initiation is closely related to the problem of unsuccessful defibrillation which has been actively studied in bidomain models (Rodríguez et al., 2005).
- *Stability*. The relative importance of filament tension, twist, and orientation, rotational anisotropy, and other effects including APD restitution, static and dynamic heterogeneity, and cardiac mechanics for filament stability in cardiac tissue remain to be established.
- *Interaction*. Interaction of filaments can be observed in numerical simulations, and preliminary studies indicate that filaments interaction depends on local gradients and the presence and chirality of other filaments (Bray and Wikswo, 2003). More work is needed to build on theoretical descriptions of filament motion (Keener and Tyson, 1992), and to establish a framework of laws that govern filament interactions.
- *Persistence*. Quantitative studies have established that many filaments are short lived, and exist for much less than one rotation of a scroll wave (Clayton and Holden, 2004a; Xie et al., 2004). It is not known whether there is an important difference in terms of overall filament interactions and dynamics between these short lived filaments (wavebreaks) and those that persist for longer.
- *Geometry*. The whole ventricle studies reported in this review indicate that the shape and anisotropy of the ventricles exert an important influence on filament behaviour, and more work is needed both to quantify this effect, and to establish any species dependence.

A key issue is how experimental and clinical observations can be related to the output of simulations. Ideally, computational simulations should be devised to answer questions that cannot be addressed experimentally; both experimental and computational studies should result in falsifiable hypotheses. Indeed a combination of experimental, clinical, and computational studies will be necessary to unravel the different strands of filament behaviour during VF. This work is critically important to gain a clearer view of the mechanisms that sustain this dangerous arrhythmia.

Acknowledgements

The work described in this was supported in part by the award of a British Heart Foundation Basic Science Lectureship to RHC, and we are grateful to the UK EPSRC and INTAS for additional financial support. We also thank A. Garfinkel for providing Fig. 7c and T. Gorissen for Fig. 6a.

Editor's note

Please see also related communications in this volume by Hervé and Sarrouilhe (2005) and Rodríguez et al. (2005).

For further downloadable content please see http://www.physiome.org.nz/publications/PBMB-2005-89/Clayton/

References

Aliev, R.R., Panfilov, A.V., 1996. Modeling of heart excitation patterns caused by a local inhomogeneity. J. Theoret. Biol. 181, 33–40.

Alonso, S., Sagues, F., Mikhailov, A.S., 2003. Taming Winfree turbulence of scroll waves in excitable media. Science 299, 1722–1725.

Antzelevitch, C., Sicouri, S., Litovsky, S.H., Lukas, A., Krishnan, S.C., Di Diego, J.M., Gintant, G.A., Liu, D.W., 1991. Heterogeneity within the ventricular wall. Electrophysiology and pharmacology of epicardial, endocardial, and M cells. Circ. Res. 69, 1427–1449.

Aslanidi, O.V., Clayton, R.H., Holden, A.V., Philips, H., Ward, R., 2003. Vulnerability to re-entry, and drift, stability, and breakdown of spiral waves in a linear gradient of GK in a Luo-Rudy1 virtual ventricular tissue. Int. J. Bifurcat. Chaos, 3865–3872.

Barnette, A.R., Bayly, P.V., Zhang, S., Walcott, G.P., Ideker, R.E., Smith, W.M., 2000. Estimation of 3-D conduction velocity vector fields from cardiac mapping data. IEEE Trans. Biomed. Eng. 47, 1027–1035.

Baxter, W.T., Mironov, S.F., Zaitsev, A.V., Jalife, J., Pertsov, A.M., 2001. Visualizing excitation waves inside cardiac muscle using transillumination. Biophys. J. 80, 516–530.

Beaumont, J., Davidenko, N., Davidenko, J.M., Jalife, J., 1998. Spiral waves in two-dimensional models of ventricular muscle: Formation of a stationary core. Biophys. J. 75, 1–14.

Berenfeld, O., Jalife, J., 1998. Purkinje-muscle reentry as a mechanism of polymorphic ventricular arrhythmias in a 3-dimensional model of the ventricles. Circ. Res. 82, 1063–1077.

Berenfeld, O., Pertsov, A.M., 1999. Dynamics of intramural scroll waves in three-dimensional continuous myocardium with rotational anisotropy. J. Theoret. Biol. 199, 383–394.

Biktashev, V.N., Holden, A.V., 1998. Re-entrant waves and their elimination in a model of mammalian ventricular tissue. Chaos 8, 48–56.

Biktashev, V.N., Holden, A.V., Zhang, H., 1994. Tension of organizing filaments of scroll waves. Philos. Trans. Roy. Soc. London Ser. A-Math. Phys. Eng. Sci. 347, 611–630.

Bray, M.-A., Wikswo, J.P., 2002a. Considerations in phase plane analysis for nonstationary reentrant cardiac behaviour. Phys. Rev. E 65, 051902-1-051902-8.

Bray, M.-A., Wikswo, J.P., 2002b. Use of topological charge to determine filament location and dynamics in a numerical model of scroll wave activity. IEEE Trans. Biomed. Eng. 49, 1086–1093.

Bray, M.-A., Wikswo, J.P., 2003. Interaction dynamics of a pair of vortex filament rings. Phys. Rev. Lett. 90, 238303-1-238303-4.

Bray, M.-A., Lin, S.-F., Aliev, R.R., Roth, B.J., Wikswo, J.P., 2001. Experimental and theoretical analysis of phase singularity dynamics in cardiac tissue. J. Cardiovasc. Electrophysiol. 12, 716–722.

Chen, P.S., Wu, T.J., Ting, C.T., Karagueuzian, H.S., Garfinkel, A., Lin, S.F., Weiss, J.N., 2003. A tale of two fibrillations. Circulation 108, 2203–2298.

Cherry, E.M., Fenton, F.H., 2004. Suppression of alternans and conduction blocks despite steep APD restitution: electrotonic, memory, and conduction velocity restitution effects. Am. J. Physiol. (Heart Circ. Physiol.) 286, H2332–H2341.

Choi, B.-R., Liu, T., Salama, G., 2001. The distribution of refractory periods influences the dynamics of ventricular fibrillation. Circ. Res. 88, e49–e58.

Choi, B.-R., Nho, W., Liu, T., Salama, G., 2002. Lifespan of ventricular fibrillation frequencies. Circ. Res. 91, 339–345.

Clayton, R.H., Holden, A.V., 2002a. Dynamics and interaction of filaments in a computational model of re-entrant ventricular fibrillation. Phys. Med. Biol. 47, 1777–1792.

Clayton, R.H., Holden, A.V., 2002b. A method to quantify the dynamics and complexity of re-entry in computational models of ventricular fibrillation. Phys. Med. Biol. 47, 225–238.

Clayton, R.H., Holden, A.V., 2003. Effect of regional differences in cardiac cellular electrophysiology in the stability of ventricular arrhythmias: A computational study. Phys. Med. Biol. 48, 95–111.

Clayton, R.H., Holden, A.V., 2004a. Filament behaviour in a computational model of ventricular fibrillation in the canine heart. IEEE Trans. Biomed. Eng. 51, 28–34.

Clayton, R.H., Holden, A.V., 2004b. Propagation of normal beats and re-entry in a computational model of ventricular cardiac tissue with regional differences in action potential shape and duration. Prog. Biophys. Mol. Biol. 85, 473–499.

Efimov, I.R., Krinsky, V.I., Jalife, J., 1995. Dynamics of rotating vortices in the Beeler-Reuter model of cardiac tissue. Chaos Solitons Fractals 5, 513–526.

Efimov, I.R., Ermentrout, B., Huang, D., Salama, G., 1996. Activation and repolarization patterns are governed by different structural characteristics of ventricular myocardium: Experimental study with voltage-sensitive dyes and numerical simulations. J. Cardiovas. Electrophysiol. 7, 512–530.

Efimov, I.R., Nikolski, V.P., Salama, G., 2004. Optical imaging of the heart. Circ. Res. 286, H2183–H2194.

Ermakova, E.A., Pertsov, A.M., Schnol, E.E., 1989. On the interaction of vortices in two dimensional active media. Physica D 40, 185–195.

Fenton, F., Karma, A., 1998a. Fiber-rotation induced vortex turbulence in thick myocardium. Phys. Rev. Lett. 81, 481–484.

Fenton, F., Karma, A., 1998b. Vortex dynamics in three-dimensional continuous myocardium with fibre rotation: Filament instability and fibrillation. Chaos 8, 20–47.

Fenton, F.H., Cherry, E.M., Hastings, H.M., Evans, S.J., 2002. Multiple mechanisms of spiral wave breakup in a model of cardiac electrical activity. Chaos 12, 852–892.

Frazier, D.W., Wolf, P.D., Wharton, J.M., Tang, A.S.L., Smith, W.M., Ideker, R.E., 1989. Stimulus induced critical point. Mechanism for electrical initiation of reentry in normal canine myocardium. J. Clin. Invest. 83, 1039–1052.

Garfinkel, A., Kim, Y.H., Voroshilovsky, O., Qu, Z.L., Kil, J.R., Lee, M.H., Karagueuzian, H.S., Weiss, J.N., Chen, P.S., 2000. Preventing ventricular fibrillation by flattening cardiac restitution. Proc. Natl. Acad. Sci. USA 97, 6061–6066.

Garny, A., Kohl, P., 2004. Mechanical induction of arrhythmias during ventricular repolarization. Modeling cellular mechanisms and their interaction in two dimensions. Ann. NY Acad. Sci. 1015, 133–143.

Garrey, W.E., 1914. Nature of fibrillatory contraction in the heart. Am. J. Physiol. 33, 397–414.

Gray, R.A., Jalife, J., 1998. Ventricular fibrillation and atrial fibrillation are two different beasts. Chaos 8, 65–78.

Gray, R.A., Jalife, J., Panfilov, A.V., Baxter, W.T., Cabo, C., Davidenko, J.M., Pertsov, A.M., 1995. Mechanisms of cardiac fibrillation. Science 270, 1222–1223.

Gray, R.A., Pertsov, A.M., Jalife, J., 1998. Spatial and temporal organization during cardiac fibrillation. Nature 392, 75–78.

Henriquez, C.S., Papazogou, A.A., 1996. Using computer models to understand the roles of tissue structure and membrane dynamics in arrhythmogenesis. Proc. IEEE 84, 334–354.

Henriquez, C.S., Tranquillo, J.V., Weinstein, D., Hsu, E.W., Johnson, C.R., 2004. Three dimensional propagation in mathematic models: Integrative model of the mouse heart. In: Zipes, D.P., Jalife, J. (Eds.), Cardiac Electrophysiology from Cell to Bedside. Saunders, Philadelphia, pp. 273–281.

Henze, C., Lugosi, E., Winfree, A.T., 1990. Helical organizing centers in excitable media. Can. J. Phys. 68, 683–710.

Hervé, J.C., Sarrouilhe, D., 2005. Protein phosphatase modulation of the intercellular junctional communication: importance in cardiac myocytes. Prog. Biophys. Mol. Biol. 89.

Hodgkin, A.L., Huxley, A.F., 1952. A quantitative description of membrane current and its application to conduction and excitation in nerve. J. Physiol. (London) 117, 500–544.

Holden, A.V., Poole, M.J., Tucker, J.V., 1996. An algorithmic model of the mammalian heart: propagation, vulnerability, re-entry and fibrillation. Int. J. Bifurcat. Chaos 6, 1623–1635.

Huikuri, H.V., Agustin, C., Myerburg, R.J., 2001. Medical progress: sudden death due to cardiac arrhythmias. N. Engl. J. Med. 345, 1473–1482.

Iyer, A.N., Gray, R.A., 2001. An experimentalist's approach to accurate localization of phase singularities during re-entry. Ann. Biomed. Eng. 29, 47–59.

Janse, M.J., Van-Cappelle, F.J.L., Morsink, H., Kleber, A.G., Wilms-Schopman, F., Cardinal, R., D'Alnoncourt, C.N., Durrer, D., 1980. Flow of "injury" currents and patterns of excitation during early ventricular arrhythmias in acute regional myocardial ischaemia in isolated porcine and canine hearts. Evidence for two different arrhythmogenic mechanisms. Circ. Res. 47, 151–165.

Karma, A., 1993. Spiral breakup in model equations of action potential propagation in cardiac tissue. Phys. Rev. Lett. 71, 1103–1107.

Keener, J.P., Bogar, K., 1998. A numerical method for the solution of the bidomain equations in cardiac tissue. Chaos 8, 234–241.

Keener, J.P., Tyson, J.J., 1992. The dynamics of scroll waves in excitable media. SIAM Rev. 34, 1–39.

Kim, Y.H., Garfinkel, A., Ikeda, T., Wu, T.J., Athill, C.A., Weiss, J.N., Karagueuzian, H.S., Chen, P.S., 1997. Spatiotemporal complexity of ventricular fibrillation revealed by tissue mass reduction in isolated swine right ventricle—Further evidence for the quasiperiodic route to chaos hypothesis. J. Clin. Invest. 100, 2486–2500.

Kleber, A.G., Rudy, Y., 2004. Basic mechanisms of cardiac impulse propagation and associated arrhythmias. Physiol. Rev. 84, 431–488.

Krinsky, V.I., Efimov, I.R., Jalife, J., 1992. Vortices with linear cores in excitable media. Proc. Roy. Soc. London A 437, 645–655.

Larson, C., Dragnev, L., Trayanova, N., 2003. Analysis of electrically induced re-entrant circuits in a sheet of myocardium. Ann. Biomed. Eng. 31, 768–780.

Lee, J.J., Kamjoo, K., Hough, D., Hwang, C., Fan, W., Fishbein, M.C., Bonometti, C., Ikeda, T., Karagueuzian, H.S., Chen, P.-S., 1996. Reentrant wave fronts in Wiggers' stage II ventricular fibrillation. Characteristics and mechanisms of termination and spontaneous regeneration. Circ. Res. 78, 660–675.

Lee, M.H., Qu, Z.L., Fishbein, G.A., Lamp, S.T., Chang, E.H., Ohara, T., Voroshilovsky, O., Kil, J.R., Hamzei, A.R., Wang, N.C., Lin, S.F., Weiss, J.N., Garfinkel, A., Karagueuzian, H.S., Chen, P.S., 2001. Patterns of wave break during ventricular fibrillation in isolated swine right ventricle. Am. J. Physiol.-Heart Circ. Physiol. 281, H253–H265.

Lewis, T., 1925. The Mechanism and Graphic Registration of the Heart Beat. Shaw and Sons Ltd, London.

Luo, C.-H., Rudy, Y., 1991. A model of the ventricular cardiac action potential. Depolarization, repolarization and their interaction. Circulation 68, 1501–1526.

Mines, G.R., 1914. On circulating excitations in heart muscles and their possible relation to tachycardia and fibrillation. Trans. Roy. Soc. Can. 4, 43–53.

Mironov, S., Vinson, M., Mulvey, S., Pertsov, A., 1996. Destabilization of three-dimensional rotating waves in an inhomogeneous BZ reaction. J. Phys. Chem. 100, 1975–1983.

Moe, G.K., Rheinboldt, W.C., Abildskov, J.A., 1964. A computer model of atrial fibrillation. Am. Heart J. 67, 200–220.

Nash, M.P., Panfilov, A.V., 2004. Electromechanical model of excitable tissue to study reentrant cardiac arrhythmias. Prog. Biophys. Mol. Biol. 85, 501–522.

Nielsen, P.M.F., LeGrice, I.J.E., Smaill, B.H., Hunter, P.J., 1991. Mathematical model of geometry and fibrous structure of the heart. Am. J. Phys. (Heart Circ. Physiol.) 29, H1365–H1378.

Noble, D., 1962. A modification of the Hodgkin-Huxley equations applicable to purkinje fibre action and pace-maker potentials. J. Physiol. 160, 317–352.

Noble, D., Rudy, Y., 2001. Models of cardiac ventricular action potentials: iterative interaction between experiment and simulation. Philos. Trans. Roy. Soc. London Ser. A-Math. Phys. Eng. Sci. 359, 1127–1142.

Panfilov, A.V., 1999. Three-dimensional organization of electrical turbulence in the heart. Phys. Rev. E 59, R6251–R6254.

Panfilov, A.V., Holden, A.V., 1993. Computer-simulation of reentry sources in myocardium in 2 and 3 dimensions. J. Theoret. Biol. 161, 271–285.

Panfilov, A., Keener, J.P., 1993a. Twisted scroll waves in heterogeneous excitable media. Int. J. Bifurcat. Chaos 3, 445–450.

Panfilov, A.V., Keener, J.P., 1993b. Generation of reentry in anisotropic myocardium. J. Cardiovasc. Electrophysiol. 4, 412–421.

Panfilov, A.V., Keener, J.P., 1995a. Re-entry in an anatomical model of the heart. Chaos Solitons Fractals 5, 681–689.

Panfilov, A.V., Keener, J.P., 1995b. Re-entry in three-dimensional Fitzhugh–Nagumo medium with rotational anisotropy. Physica D 84, 545–552.

Panfilov, A.V., Pertsov, A.M., 2001. Ventricular fibrillation: evolution of the multiple-wavelet hypothesis. Philos. Trans. Roy. Soc. London Ser. A-Math. Phys. Eng. Sci. 359, 1315–1325.

Panfilov, A.V., Rudenko, A.N., 1987. Two regimes of the scroll ring drift in the three-dimensional active media. Physica D 28, 215–218.

Panfilov, A.V., Rudenko, A.N., Pertsov, A.M., 1984. Twisted scroll waves in three- dimensional active media. Rep. Acad. Sci. USSR (Doklady AN SSSR) 279, 1000–1002.

Panfilov, A.V., Rudenko, A.N., Krinsky, V.I., 1986. Scroll rings in three-dimensional active medium with two component diffusion. Biofizika 31, 850–854.

Pertsov, A., Vinson, M., Muller, S.C., 1993. 3-Dimensional reconstruction of organizing centers in Excitable chemical media. Physica D 63, 233–240.

Pertsov, A.M., Wellner, M., Vinson, M., Jalife, J., 2000. Topological constraint on scroll wave pinning. Phys. Rev. Lett. 84, 2738–2741.

Priori, S.G., Aliot, E., Blomstrom-Lundqvist, C., Bossaert, L., Breithardt, G., Brugada, P., Camm, A.J., Cappato, R., 2001. Task force on sudden cardiac death of the European Society of Cardiology. Eur. Heart J. 22, 1374–1450.

Qu, Z.L., Kil, K., Xie, F.G., Garfinkel, A., Weiss, J.N., 2000. Scroll wave dynamics in a three-dimensional cardiac tissue model: roles of restitution, thickness, and fiber rotation. Biophys. J. 78, 2761–2775.

Rappel, W.-J., 2001. Filament instability and rotational anisotropy: a numerical study using detailed cardiac models. Chaos 11, 71–80.

Rodríguez, B., Eason, J.C., Trayanova, N., 2005. Differences between left and right ventricular anatomy determine the types of reentrant circuits induced by an external electric shock. A rabbit heart simulation study. Prog. Biophys. Mol. Biol. 89.

Rogers, J.M., 2002. Wave front fragmentation due to ventricular geometry in a model of the rabbit heart. Chaos 12, 779–787.

Rogers, J.M., Ideker, R.E., 2000. Fibrillating myocardium. Rabbit warren or beehive? Circulation 86, 369–370.

Rogers, J.M., Huang, J., Smith, W.M., Ideker, R.E., 1999. Incidence, evolution, and spatial distribution of functional reentry during ventricular fibrillation in pigs. Circ. Res. 84, 945–954.

Roth, B.J., 2004. Art Winfree and the bidomain model of cardiac tissue. J. Theoret. Biol. 230, 445–449.

Rudenko, A.N., Panfilov, A.V., 1983. Drift and interaction of vortices in two dimensional heterogenous active medium. Stud. Biophys. 98.

Sambelashvilli, A., Efimov, I.R., 2004. Dynamics of virtual electrode-induced scroll-wave reentry in a 3D bidomain model. Am. J. Physiol. (Heart Circ. Physiol.) 287, H1570–H1581.

Samie, F.H., Berenfeld, O., Anumono, J., Mironov, S., Udassi, S., Beaumont, J., Taffet, S., Pertsov, A., Jalife, J., 2001. Rectification of the background potassium current. A determinant of rotor dynamics in ventricular fibrillation. Circ. Res. 89, 1216–1223.

Stevens, C., Remme, E., LeGrice, I.J., Hunter, P.J., 2003. Ventricular mechanics in diastole: material parameter sensitivity. J. Biomech. 36, 737–748.

Storb, U., Neto, C.R., Bar, M., Muller, S.C., 2003. A tomographic study of desynchronization and complex dynamics of scroll waves in an excitable chemical reaction with a gradient. Phys. Chem. Chem. Phys. 5, 2344–2353.

Streeter, D.D., 1979. Gross morphology and fibrous structure of the heart. In Handbook of Physiology—The Cardiovascular System, vol. 1, American Physiological Society, Baltimore, pp. 61–112.

Surawicz, B., 2003. Brief history of cardiac arrhythmias since the end of the nineteenth century: Part 1. J. Cardiovasc. Electrophysiol. 14, 1365–1371.

Surawicz, B., 2004. Brief history of cardiac arrhythmias since the end of the nineteenth century: Part 2. J. Cardiovasc. Electrophysiol. 15, 101–111.

TenTusscher, K.H.W.J., Panfilov, A.V., 2003. Re-entry in heterogeneous cardiac tissue described by the Luo–Rudy ventricular action potential model. Am. J. Physiol. (Heart Circ. Physiol.) 284, H542–H548.

TenTusscher, K.H.W.J., Panfilov, A.V., 2004. Eikonal formulation of the minimal principle for scroll wave filaments. Phys. Rev. Lett. 93, 108106-1–108106-4.

Trayanova, N.A., Eason, J.C., Aguel, F., 2002. Computer simulations of cardiac defibrillation: a look inside the heart. Comput. Visualization Sci. 4, 259–270.

Valderrabano, M., Yang, J., Omichi, C., Kil, J.R., Lamp, S.T., Qu, Z.L., Lin, S.-F., Karagueuzian, H.S., Garfinkel, A., Chen, P.S., Weiss, J., 2002. Frequency analysis of ventricular fibrillation in swine ventricles. Circ. Res. 90, 213–222.

Vetter, F.J., McCulloch, A.D., 1998. Three dimensional analysis of regional cardiac function: A model of rabbit ventricular anatomy. Prog. Biophys. Mol. Biol. 69, 157–183.

Wellner, O., Berenfeld, O., Jalife, J., Pertsov, A., 2002. Minimal principle for rotor filaments. Proc. Natl. Acad. Sci. 99, 8015–8018.

Wiggers, C.J., 1940. The mechanism and nature of ventricular fibrillation. Am. Heart J. 20, 399–412.

Winfree, A.T., 1973. Scroll-shaped waves of chemical activity in three dimensions. Science 181, 937–939.

Winfree, A.T., 1991. Varieties of spiral wave behaviour in excitable media. Chaos 1, 303–334.

Winfree, A.T., Strogatz, S.H., 1984. Organizing centres for three dimensional chemical waves. Nature 311, 611–615.

Winfree, A.T., Caudle, S., Chen, G., McGuire, P., Szilagyi, Z., 1996. Quantitative optical tomography of chemical waves and their organizing centres. Chaos 6, 617–626.

Witkowski, F.X., Leon, L.J., Penkoske, P.A., Giles, W.R., Spano, M.L., Ditto, W.L., Winfree, A.T., 1998. Spatiotemporal evolution of ventricular fibrillation. Nature 392, 78–82.

Wolk, R., Cobbe, S.M., Kane, K.A., Hicks, M.N., 1999. Relevance of inter- and intraventricular electrical dispersion to arrhythmogenesis in normal and ischaemic rabbit myocardium: A study with Cromalkim, 5-Hydroxydecanoate and Glibenclamide. J. Cardiovasc. Pharmacol. 33, 323–334.

Wu, T.J., Lin, S.F., Weiss, J.N., Ting, C.T., Chen, P.S., 2002. Two types of ventricular fibrillation in isolated rabbit hearts. Importance of excitability and action potential restitution. Circulation 106, 1859–1866.

Xie, F., Qu, Z.L., Yang, J., Baher, A., Weiss, J.N., Garfinkel, A., 2004. A simulation study of the effects of cardiac anatomy in ventricular fibrillation. J. Clin. Invest. 113, 686–693.

Zykov, V.S., 1986. Cycloidal circulation of spiral waves in excitable media. Biofizika 31, 862–865.